



Exome Sequencing Links Corticospinal Motor Neuron Disease to Common Neurodegenerative Disorders

Gaia Novarino *et al.*
Science **343**, 506 (2014);
DOI: 10.1126/science.1247363

This copy is for your personal, non-commercial use only.

If you wish to distribute this article to others, you can order high-quality copies for your colleagues, clients, or customers by [clicking here](#).

Permission to republish or repurpose articles or portions of articles can be obtained by following the guidelines [here](#).

The following resources related to this article are available online at www.sciencemag.org (this information is current as of February 12, 2014):

Updated information and services, including high-resolution figures, can be found in the online version of this article at:

<http://www.sciencemag.org/content/343/6170/506.full.html>

Supporting Online Material can be found at:

<http://www.sciencemag.org/content/suppl/2014/01/30/343.6170.506.DC1.html>

A list of selected additional articles on the Science Web sites **related to this article** can be found at:

<http://www.sciencemag.org/content/343/6170/506.full.html#related>

This article **cites 51 articles**, 18 of which can be accessed free:

<http://www.sciencemag.org/content/343/6170/506.full.html#ref-list-1>

This article has been **cited by** 1 articles hosted by HighWire Press; see:

<http://www.sciencemag.org/content/343/6170/506.full.html#related-urls>

This article appears in the following **subject collections**:

Genetics

<http://www.sciencemag.org/cgi/collection/genetics>

Exome Sequencing Links Corticospinal Motor Neuron Disease to Common Neurodegenerative Disorders

Gaia Novarino,^{1*†} Ali G. Fenstermaker,^{1*} Maha S. Zaki,^{3*} Matan Hofree,² Jennifer L. Silhavy,¹ Andrew D. Heiberg,¹ Mostafa Abdellateef,¹ Basak Rosti,¹ Eric Scott,¹ Lobna Mansour,⁴ Amira Masri,⁵ Hulya Kayserili,⁶ Jumana Y. Al-Aama,⁷ Ghada M. H. Abdel-Salam,³ Ariana Karminejad,⁸ Majdi Kara,⁹ Bulent Kara,¹⁰ Bita Bozorgmehr,⁸ Tawfeq Ben-Omran,¹¹ Faezeh Mojahedi,¹² Iman Gamal El Din Mahmoud,⁴ Naima Bouslam,¹³ Ahmed Bouhouche,¹³ Ali Benomar,¹³ Sylvain Hanein,¹⁴ Laure Raymond,¹⁴ Sylvie Forlani,¹⁴ Massimo Mascaro,¹ Laila Selim,⁴ Nabil Shehata,¹⁵ Nasir Al-Allawi,¹⁶ P.S. Bindu,¹⁷ Matloob Azam,¹⁸ Murat Gunel,¹⁹ Ahmet Caglayan,¹⁹ Kaya Bilguvar,¹⁹ Aslihan Tolun,²⁰ Mahmoud Y. Issa,³ Jana Schroth,¹ Emily G. Spencer,¹ Rasim O. Rosti,¹ Naiara Akizu,¹ Keith K. Vaux,¹ Anide Johansen,¹ Alice A. Koh,¹ Hisham Megahed,³ Alexandra Durr,^{14,21} Alexis Brice,^{14,21,22} Giovanni Stevanin,^{14,21,22,23} Stacy B. Gabriel,²⁴ Trey Ideker,² Joseph G. Gleeson^{1‡}

Hereditary spastic paraplegias (HSPs) are neurodegenerative motor neuron diseases characterized by progressive age-dependent loss of corticospinal motor tract function. Although the genetic basis is partly understood, only a fraction of cases can receive a genetic diagnosis, and a global view of HSP is lacking. By using whole-exome sequencing in combination with network analysis, we identified 18 previously unknown putative HSP genes and validated nearly all of these genes functionally or genetically. The pathways highlighted by these mutations link HSP to cellular transport, nucleotide metabolism, and synapse and axon development. Network analysis revealed a host of further candidate genes, of which three were mutated in our cohort. Our analysis links HSP to other neurodegenerative disorders and can facilitate gene discovery and mechanistic understanding of disease.

Hereditary spastic paraplegias (HSPs) are a group of genetically heterogeneous neurodegenerative disorders with prevalence between 3 and 10 per 100,000 individuals (1). Hallmark features are axonal degeneration and progressive lower limb spasticity resulting from a loss of corticospinal tract (CST) function. HSP is classified into two broad categories, uncomplicated and complicated, on the basis of the presence of additional clinical features such as intellectual disability, seizures, ataxia, peripheral neuropathy, skin abnormalities, and visual defects. The condition displays several distinct modes of inheritance, including autosomal dominant, autosomal recessive, and X-linked. Several loci have been linked to autosomal recessive HSP (AR-HSP), from which 22 genes with mutations have been cloned. However, most of the underlying causes of HSP remain unidentified.

We analyzed 55 families displaying AR-HSP by whole-exome sequencing (WES). We identified the genetic basis in about 75% of the cases, greatly increasing the number of mutated genes in HSP; functionally validated many of these genes in zebrafish; defined new biological processes underlying HSP; and created an “HSPome” interaction map to help guide future studies.

Multiple Genes Are Implicated in HSP

We used WES to identify the genetic causes of AR-HSP in families with documented consanguinity. Selecting from these families without

congenital malformations referred for features of either complicated or uncomplicated HSP (table S1), we performed WES on 93 individuals typically from two affected siblings or cousins where possible, for multiplex families, or one affected and one unaffected sibling or both parents, for simplex families. We prioritized predicted protein frame shift, stop codon, splice defects, and conserved nonsynonymous amino acid substitution mutations [Genomic Evolutionary Rate Profile (GERP) score > 4 or phastCons (genome conservation) score > 0.9]. We excluded variants with an allele frequency of greater than 0.2% in our internal exome database of over 2000 individuals. We genotyped each informative member from the majority of families with a 5000 single-nucleotide polymorphism (SNP) panel and generated genome-wide parametric multipoint linkage plots or used WES data to generate homozygosity plots (2). We excluded variants falling outside of homozygous intervals <2.0 Mb threshold (fig. S1).

We tested segregation of every variant meeting these criteria (table S2). We report a candidate HSP gene only if there was a single deleterious variant that segregated in the family or if the gene was identified as mutated in multiple families (3). For 15 families, a single genetic cause could not be identified. We identified mutations in 13 genes known to be mutated in HSP (33% of the cases in our cohort) (table S3 and fig. S2), supporting the methodology. These include *EIF2B5*, associated with vanishing white-matter disease [Online Men-

delian Inheritance in Man (OMIM) no. 603896]; *CLN8*, associated with ceroid lipofuscinosis (OMIM 600143); and *ARG1*, which causes arginase deficiency (OMIM 207800). The diversity of genes identified speaks to the heterogeneity of HSP presentations. *ALS2* (OMIM 205100) was mutated in four different families presenting with uncomplicated HSP, and *ATL1* (OMIM 182600) was mutated in three different families, some displaying partial penetrance (4).

We identified 14 candidate genes not previously implicated in disease (Table 1), accounting for 42% of the cases in our cohort. We also evaluated five non-consanguineous families by WES, implicating one additional candidate gene. We estimated, on the basis of our false discovery rate (FDR), that fewer than 0.1 alleles per family should pass this threshold randomly, dependent on the number of informative meioses, suggesting that fewer than 1:10 genes identified with this method should prove false positive (i.e., identify by chance) (3).

The mutations in the 15 novel genes were identified in patients presenting with a spectrum of HSP phenotypes. Three of these genes, *ERLIN1*,

¹Howard Hughes Medical Institute, University of California, San Diego, La Jolla, CA 92093, USA. ²Department of Computer Science and Engineering and Department of Medicine, University of California, San Diego, La Jolla, CA 92093, USA. ³Clinical Genetics Department, Human Genetics and Genome Research Division, National Research Center, Cairo 12311, Egypt. ⁴Department of Pediatric Neurology, Neurometabolic Unit, Cairo University Children's Hospital, Cairo 406, Egypt. ⁵Division of Child Neurology, Department of Pediatrics, University of Jordan, Amman 11942, Jordan. ⁶Istanbul University, Istanbul Medical Faculty, Medical Genetics Department, 34093 Istanbul, Turkey. ⁷Department of Genetic Medicine, King Abdulaziz University, Jeddah, Kingdom of Saudi Arabia. ⁸Kariminejad-Najmabadi Pathology and Genetics Center, Tehran, Iran. ⁹Department of Pediatrics, Tripoli Children's Hospital, Tripoli, Libya. ¹⁰Kocaeli University, Medical Faculty, Department of Pediatric Neurology, 41380 Umutepe, Kocaeli, Turkey. ¹¹Clinical and Metabolic Genetics Division, Department of Pediatrics, Hamad Medical Corporation, Doha 3050, Qatar. ¹²Mashhad Medical Genetic Counseling Center, 91767 Mashhad, Iran. ¹³Université Mohammed V Souissi, Equipe de Recherche de Maladies Neuro-dégénératives (ERMN) and Centre de Recherche en Épidémiologie Clinique et Essais Thérapeutiques (CRCEET), 6402 Rabat, Morocco. ¹⁴Centre de Recherche de l'Institut du Cerveau et de la Moelle épinière, INSERM U1127, CNRS UMR7225; UPMC Univ Paris VI UMR S975, 75013 Paris, France. ¹⁵Department of Pediatrics and Neonatology, Saudi German Hospital, Post Office Box 84348, Riyadh, Kingdom of Saudi Arabia. ¹⁶Department of Pathology, School of Medicine, University of Dohuk, Dohuk, Iraq. ¹⁷Department of Neurology, National Institute of Mental Health and Neurosciences, Bangalore, India. ¹⁸Department of Pediatrics and Child Neurology, Wah Medical College, Wah Cantt, Pakistan. ¹⁹Department of Genetics and Neurosurgery, Yale University School of Medicine, New Haven, CT 06510, USA. ²⁰Department of Molecular Biology and Genetics, Bogazici University, 34342 Istanbul, Turkey. ²¹Assistance Publique–Hôpitaux de Paris, Fédération de Génétique, Pitié-Salpêtrière Hospital, 75013 Paris, France. ²²Institut du Cerveau et de la Moelle épinière, 75013 Paris, France. ²³Laboratoire de Neurogénétique, Ecole Pratique des Hautes Etudes, Institut du Cerveau et de la Moelle épinière, 75013 Paris, France. ²⁴Broad Institute of Harvard and Massachusetts Institute of Technology, Cambridge, MA 02142, USA.

*These authors contributed equally to this work.

†Present address: IST Austria (Institute of Science and Technology Austria), Klosterneuburg, Austria.

‡Corresponding author. E-mail: jogleeson@ucsd.edu

KIF1C, and *NT5C2*, were found independently mutated in more than one family, and all mutations were predicted to be highly deleterious. All but one was homozygous, whereas the non-consanguineous family 787, with four affected and six healthy children, displayed a compound heterozygous mutation. This approach thus identified a host of novel candidate genes for further investigation.

Extending Results to Larger HSP Cohort

An additional cohort of 200 patients diagnosed with HSP (5) were screened for mutations in these genes with exome sequencing or microfluidic polymerase chain reaction (PCR) followed by sequencing (3). Additional mutations in *ERLIN1*, *ENTPD1*, *KIF1C*, *NT5C2*, and *DDHD2* were identified (Table 1), thus validating these in the pathogenesis of HSP. Microfluidic PCR provided threshold coverage of only 68% of the targeted exons, suggesting that improved methods will be required to fully evaluate this second cohort. While this paper was in preparation, *DDHD2* was published as mutated in complicated HSP, cross-validating results (6).

Functional Testing Candidates with Expression and Zebrafish

To understand the potential role of these disease genes in HSP, we profiled their expression across multiple human tissues with reverse transcription PCR. Expression was specific to neural tissue for

the genes *FLRT1* and *ZFR*, suggesting a neuronal function (fig. S3). For most, however, we noted broadly distributed expression patterns, suggesting functions in other tissues but that neurons show increased susceptibility to genetic mutations.

To functionally validate the private genes (i.e., those mutated in a single family), we performed knockdown modeling in zebrafish. Phylogenetic analysis indicated a single zebrafish ortholog for the private genes *ARL6IP1*, *MARS*, *PGAP1*, and *USP8*. Morphants were phenotyped for lethality and defects in body axis (Fig. 1 and fig. S4), motor neuron morphology (fig. S5), and evoked and spontaneous swimming behavior, all relevant to HSP. Except for *mars* morphants, which were too severe to be analyzed completely, we identified phenotypes for all morphants in both touch-induced and spontaneous locomotion behavior, as previously reported for other HSP candidate genes (7). Although more work is warranted to conclusively uncover the role of the tested genes in CST degeneration, our *in vivo* functional validation supports the genetic data.

HSP-Related Proteins Interact Within a Network

To generate an HSPome containing all known and candidate genes as well as proximal interactors, we first created a protein network of all known human genes and/or proteins. We then extracted the subnetwork containing all previously published HSP mutated genes (seeds, table S4) to

derive the HSP seeds network and then extracted the subnetwork containing all seed genes plus candidate HSP genes (from Table 1) to derive the HSP seed + candidates network (Fig. 2A).

We tested whether the HSP seeds network was more highly connected than expected by chance. We compared the connectivity of the network comparing the 43 seeds to a background network generated by 10,000 permutations of randomly selected sets of 43 seeds from the global network using three different measures of connectivity: (i) the number of edges within the query set (within group edge count), (ii) the mean overlap in interaction neighborhoods between pairs of proteins in the query set (Jaccard similarity), and (iii) the mean random walk similarity (i.e., the expected “time” it takes to get from one protein to another when performing a random walk on the network) (8). By all three measures, we found the HSP seed proteins were more cohesive than expected at random ($P = 2.0 \times 10^{-04}$, $P = 1.3 \times 10^{-03}$, and $P = 1.5 \times 10^{-05}$) (Fig. 2B and supplementary data 1).

We also examined whether the HSP seed + candidates network, containing 43 seeds plus 15 candidates, was more highly connected than expected in a background of 10,000 random permutations (Fig. 2C). The addition of the candidates to the HSP seeds network resulted in a set significantly more highly connected than expected by chance ($P = 3.1 \times 10^{-02}$, $P = 1.2 \times 10^{-03}$, $P = 4.8 \times 10^{-04}$, respectively). We conclude that these newly

Table 1. Novel candidate HSP genes. List of novel candidate HSP genes identified through WES, divided into major functional modules (ERAD, etc.). OMIM nomenclature refers to established or new (beginning with SPG58) locus. Position refers to the Genome Browser release 19 map. Family 787 has a compound heterozygous mutation in the *MARS* gene. C, complicated; U, uncomplicated forms

Gene Symbol	Locus Nomenclature	Entrez Gene ID	Gene Name	Putative Biological Function	Family #	Position (hg19)	Nucleotide Change	Deduced Protein Change	Effect on Protein	Phenotype
Endoplasmic reticulum and ER-associated degradation (ERAD)										
<i>ARL6IP1</i>	<i>SPG61</i>	23204	ADP-ribosylation factor-like 6 interacting protein 1	Protein transport	827	chr16:18804609 TGTTT>T	c.576_579delAAAC	p.K193Ffs36X	Frameshift	C
<i>ERLIN1</i>	<i>SPG62</i>	10613	ER lipid raft associated 1	ER-associated degradation	786 1098 1598	chr10:101914679 G>A chr10:101943559 C>A chr10:101912067 CCTGGTA>C	c.C783T c.G149T c.862_868delACCAGG	p.R255X p.G50V p.del203-204YQ	Stop codon Missense Frameshift	U U U
Endosome and membrane trafficking										
<i>KIF1C</i>	<i>SPG58</i>	10749	Kinesin family member 1C	Retrograde Golgi to ER transport	789 803	chr17:4904143 G>A chr17:4925567 C>T	c.G183A c.C2191T	Splice p.R731X	N/A Stop codon	C U
<i>USP8</i>	<i>SPG59</i>	9101	Ubiquitin specific peptidase 8	Deubiquitinating enzyme	882	chr15:50769124 C>A	c.C928A	p.Q310K	Missense	C
<i>WDR48</i>	<i>SPG60</i>	57599	WD repeat domain 48	Regulator of deubiquitination	910	chr3:39135498 AAAG>A	c.1879_1881delAAG	p.del628E	Amino acid del	C
Nucleotide metabolism										
<i>AMPD2</i>	<i>SPG63</i>	271	Adenosine monophosphate deaminase 2	Deaminates AMP to IMP in purine nucleotide metabolism	1526	chr1:110167989 CT>C	c.318delT	p.C107Afs365X	Frameshift	C
<i>ENTPD1</i>	<i>SPG64</i>	953	Ectonucleoside triphosphate diphosphohydrolase 1	Hydrolyzes ATP and other nucleotides to regulate purinergic transmission	1242 1800	chr10:97605168 G>A chr10:97604339 G>T	c.G649A c.G719T	p.G217R p.E181X	Missense Stop codon	C C
<i>NT5C2</i>	<i>SPG65</i>	22978	5'-nucleotidase, cytosolic II	Preferentially hydrolyzes IMP, in both purine/pyrimidine nucleotide metabolism	659 1290 1549 1829	chr10:104899162 C>T chr10:104850739 CT>C chr10:104853067 C>A chr10:104834653 C>T chr10:104861028 T>A	c.175+1G>A c.1225delA c.988-1G>T c.G86A c.A445T	Splice p.S409Vfs436X p.988-1G>T p.R29X p.R149X	N/A Frameshift N/A Stop codon Stop codon	U C U U C
Lipid/Myelination related										
<i>ARSI</i>	<i>SPG66</i>	340075	Arylsulfatase family, member I	Hydrolyze sulfate esters Hormone biosynthesis	1349	chr5:149676845 A>AT	c.1641insA	p.C548Mfs559X	Frameshift	C
<i>DDHD2</i>	<i>SPG54</i>	23259	DDHD domain-containing protein 2	Phospholipase preferentially hydrolyzes phosphatidic acid	1675 1314	chr8:38103473 C>G chr8:38103270 C>T	c.1057+5C>G c.C859T	Splice p.R287X	N/A Stop codon	C C
<i>PGAP1</i>	<i>SPG67</i>	80055	Post-GPI attachment to proteins 1	GPI biosynthesis	1241	chr2:197712670 C>A	c.1952+1G>T	Splice	N/A	C
Axon guidance/synapse related										
<i>FLRT1</i>	<i>SPG68</i>	23769	Fibronectin leucine rich transmembrane protein 1	Cell adhesion and receptor signaling	709	chr11:63885762 T>C	c.T2023C	Stop-loss	Stop-loss	C
<i>RAB3GAP2</i>	<i>SPG69</i>	25782	RAB3 GTPase activating protein subunit 2	Exocytosis of neurotransmitters and hormones	738	chr1:220357421 A>C	c.T1955G	p.L252X	Stop codon	C
Other										
<i>MARS</i>	<i>SPG70</i>	4141	Methionyl-tRNA synthetase	Cytosolic methionyl-tRNA synthetase	787	chr12:57881886 G>A chr12:57908741 C>T	c.G13A;c.C2104T	p.V5M;p.R702W	Missense Missense	C C
<i>ZFR</i>	<i>SPG71</i>	51663	Zinc finger RNA binding protein	RNA localization?	1611	chr5:32406955 A>G	c.T956C	p.L319P	Missense	U

of HSP. ADP, adenosine diphosphate; IMP, inosine monophosphate; ATP, adenosine triphosphate; DDHD, Asp-Asp-His domain; GPI, glycosyl phosphatidylinositol; GTPase, guanosine triphosphatase; tRNA, transfer RNA. N/A, not applicable. Single-letter amino acid abbreviations are as follows: C, Cys; E, Glu; F, Phe; G, Gly; I, Ile; K, Lys; L, Leu; P, Pro; Q, Gln; R, Arg; S, Ser; T, Thr; V, Val; and X, termination.

identified genes are more cohesive than would be expected with candidates selected at random.

To identify proximal interactors, we expanded the global network by including HumanNet protein interaction database (9) and literature-curated interactions from STRING (10) to derive an expanded global network (fig. S6). This network propagation method assigns a priority score to each protein within the network (11). From this expanded network, we extracted the expanded HSP seeds network and found that 7 of the 15 newly identified candidates have significant support in the network (*ARSI*, *DDHD2*, *ERLIN1*, *FLRT1*, *KIF1C*, *PGAP1*, and *RAB3GAP2*, FDR < 0.1). Genes involved in biochemical pathways, such as *NT5C2*, *AMPD2*, and *ENTPD1*, did not emerge from this analysis, probably because of a lack of metabolic network edges in the input networks. Proteins that were not well characterized or represented in public databases also did not show enrichment.

We next expanded the HSP seed + candidate network to derive the HSPome (i.e., HSP seeds + candidates + proximal interactors network), allowing a global view of HSP and flagging other potential genes that may be mutated in HSP patients. The HSPome contains 589 proteins (i.e., potential HSP candidates) (supplementary data 2 and table S5).

Implicated Causal Genes Suggest Modules of HSP Pathology

Studies in HSP consistently report an ascending axonal CST degeneration (12), but the processes modulating this degeneration are not well defined. Supporting the hypothesis that individual rare mutations in distinct genes may converge on specific biological pathways, we identified major modules involved in the pathophysiology of HSP. Several HSP genes have previously implicated endoplasmic reticulum (ER) biology (i.e., *ATL1*, *REEP1*, *RTN2*, and *SPAST*) and the ER-associated

degradation (ERAD) pathway (i.e., *ERLIN2*) (13–15). From the HSPome, we focused on this ER subnetwork containing the newly identified genes *ARL6IP1* and *ERLIN1* (fig. S7). *ARL6IP1* encodes a tetraspan membrane protein localized to the ER, composed of highly conserved hydrophobic hairpin domains implicated in the formation of ER tubules (16). We overexpressed *ARL6IP1* in cells and noted dramatically altered ER shape (fig. S7). The ERAD system controls protein quality control, critical for cellular adaptation to stress and survival. *ERLIN1* encodes a prohibitin-domain-containing protein localized to the ER that forms a ring-shaped complex with *ERLIN2*, further implicating defective ERAD in HSP etiology.

We identified an endosomal and membrane-trafficking subnetwork composed of seeds and candidates *KIF1C*, *USP8*, and *WDR48*, implicating the endosomal sorting complexes required for transport (ESCRT) pathway (fig. S8). *USP8*

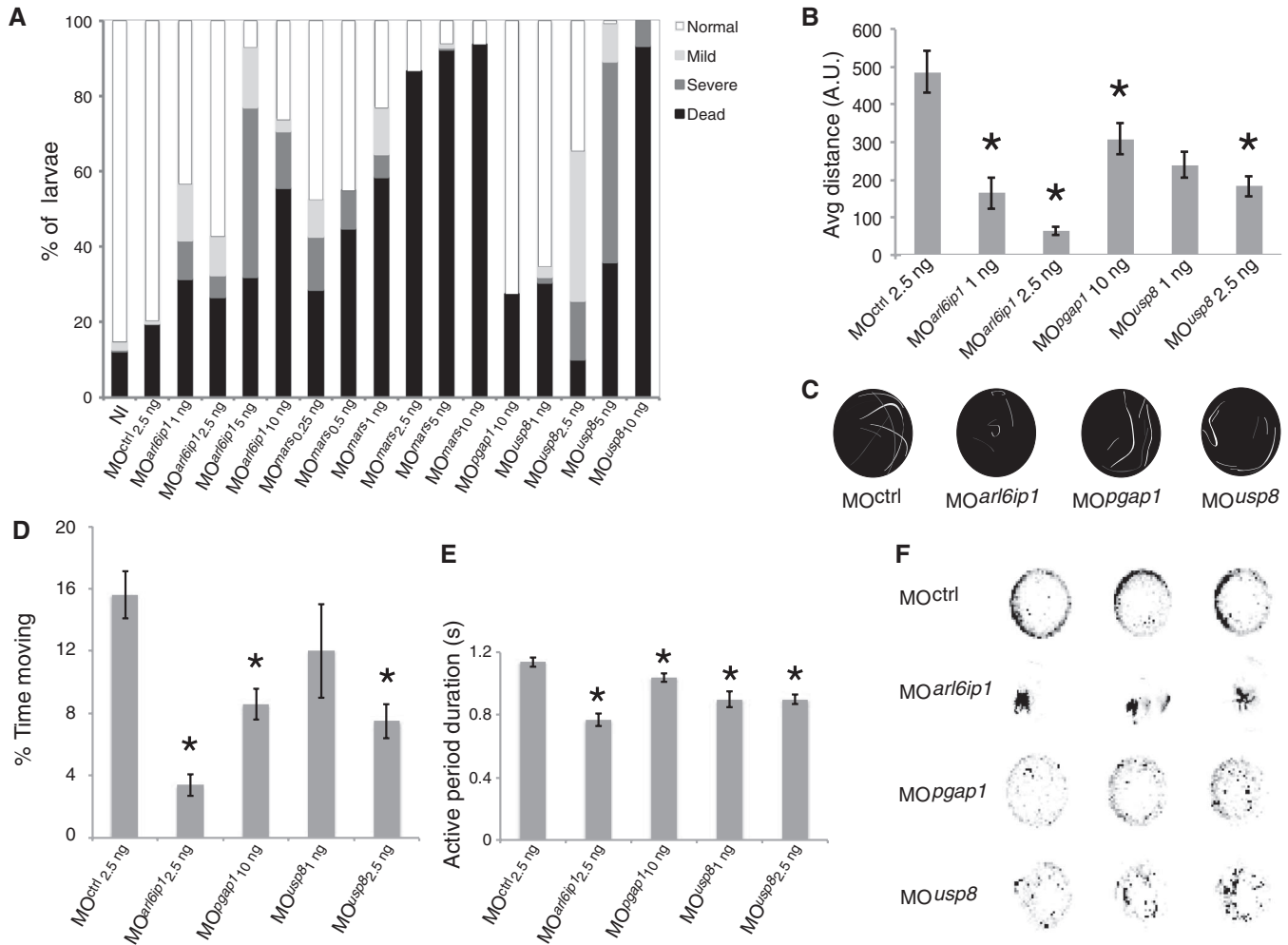


Fig. 1. Functional validation of private HSP genes in zebrafish. (A) Quantification of 24-hours-post-fertilization (hpf) embryos mortality (black) and curly-tail (gray) phenotypes for noninjected (NI), scrambled, and morphants (MO) at stated nanogram concentrations. Overt phenotypes were observed for all MOs except *MOpgap1*. (B) Average touch-response distance (in arbitrary units, A.U.) in 72-hpf larvae, showing blunted response for all MOs. (C) Immediate touch-response trajectory of example larvae, each shaded uniquely. *Mars2* MO was too severe to be tested, whereas others showed reduced response.

(D to F) Spontaneous locomotion at 6 days post fertilization. (D) Average percent of time spent moving over a 30-min window showed a reduction for all for at least one dose. (E) Average active period duration, showing reduction for all. (F) Representative kymographs recording fish position (black dot) over 30-min recording. MOs showed either short distance traveled (*MOarl6ip1*) or reduced movements per recording (*MOpgap1* and *MOusp8*). * $p < 0.01$ (t test). $N > 2$ experiments with $n > 20$ animals per experiment. Error bars indicate standard error.

encodes a deubiquitinating enzyme (DUB) in the ESCRT pathway (17). The *WDR48*-encoded protein forms stable complexes with multiple DUBs, such as USP1, USP12, and USP46, and is required for enzymatic activity and linked to lysosomal trafficking (18, 19). *KIF1C* encodes a motor protein localized to the ER/Golgi complex, suggesting a role in trafficking (20). To validate the effect of the putative splicing mutation in family 789, we obtained fibroblasts and confirmed skipping of exon 4 (fig. S9). Defects in ESCRT are linked to neurodegenerative disorders such as frontotemporal dementia, Charcot Marie Tooth disease, and recently AR-HSP (21–23). Additionally, the HSP gene products SPG20, SPAST, and ZFYVE26 interact with components of this complex (24–26). Taken together, this suggests that disruptions in ESCRT and endosomal function can lead to HSP and other forms of neurodegeneration.

AMPD2, *ENTPD1*, and *NT5C2* are involved in purine nucleotide metabolism (fig. S10). Nucleotide metabolism is linked to the neurological disorder Lesch-Nyhan disease, among others (27), but was not previously implicated in HSP. *AMPD2*

encodes one of three adenosine monophosphate (AMP) deaminase enzymes involved in balancing purine levels (28). Mutations in *AMPD2* have been recently linked to a neurodegenerative brainstem disorder (28). In addition, the deletion we have identified in this study affects just the longest of the three *AMPD2* isoforms, indicating that the most N-terminal domain of *AMPD2* is important to prevent motor neuron degeneration. *ENTPD1* encodes an extracellular ectonuclease hydrolyzing adenosine nucleotides in the synaptic cleft (29). *NT5C2* encodes a downstream cytosolic purine nucleotide 5' phosphatase. Purine nucleotides are neuroprotective and play a critical role in the ischemic and developing brain (29); thus, alterations in their levels could sensitize neurons to stress and insult. *ENTPD1* was recently identified as a candidate gene in a family with nonsyndromic intellectual disability, but *HSP* was not evaluated (30).

Candidate HSP Genes Identified by Network Analysis

For families that were not included in our initial analysis, we interrogated our exome database for

variants in genes emerging from the extended HSPome network. By using this method, we identified potentially pathogenic variants in *MAG*, *BICD2*, and *REEP2*, found in homozygous intervals in three families (Fig. 3), validating the usefulness of the HSPome to identify new HSP genes. Interacting with *KIF1C* in the HSPome is *CCDC64*, encoding a member of the Bicaudal family (31), a paralog of the *BIC2* gene that emerged in the HSPome (FDR < 0.05, table S5). Family 1370 displays a homozygous Ser⁶⁰⁸→Leu⁶⁰⁸ missense change in the *BIC2* gene within a homozygous haplotype. The *Drosophila* bicaudal-D protein is associated with Golgi-to-ER transport and potentially regulates the rate of synaptic vesicle recycling (32). Coimmunoprecipitation confirmed that *BICD2* physically interacts with *KIF1C* (fig. S11). Recently, a mutation in *BICD2* was implicated in a dominant form of HSP (33).

MAG was identified as a significant potential HSP candidate (FDR < 0.05) from the HSPome, interacting with *PLP1*, the gene product mutated in *SPG2*. *MAG* is a membrane-bound adhesion protein implicated in myelin function, and knockout

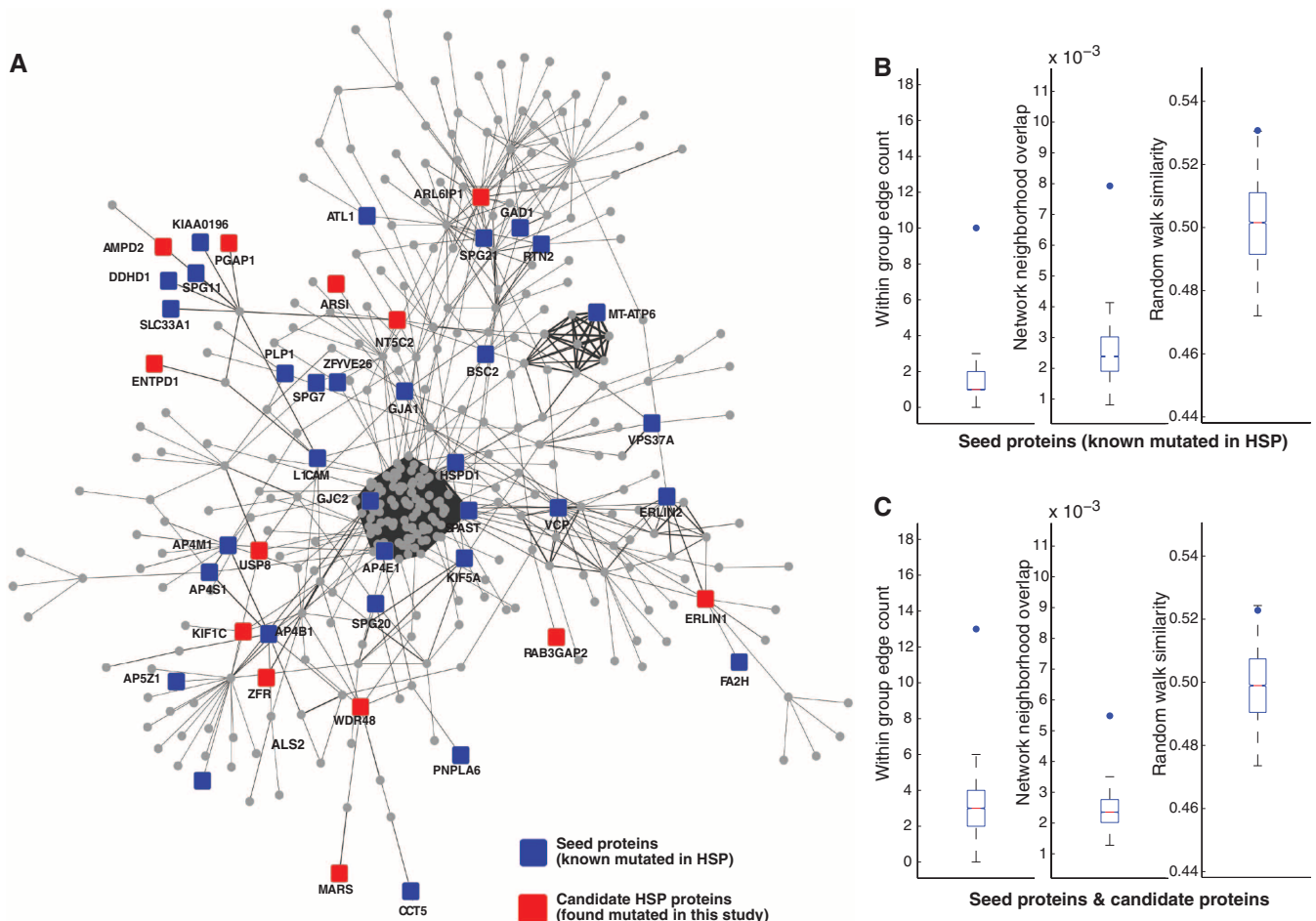


Fig. 2. Hereditary spastic paraplegia interactome. (A) HSP seeds + candidate network (edge-weighted force-directed layout), demonstrating many of the genes known to be mutated in HSP (seeds, blue) and new HSP candidates (red), along with others (circles) constituting the network. (B and C) Comparison of statistical strength of HSP subnetworks with 10,000 permutations of randomly selected proteins. Dots denote the value of the metric on the true set (i.e., seeds

or seeds + candidates). Box and whisker plots denote matched null distributions (i.e., 10,000 permutations). (B) Seed (known mutated in HSP) versus random proteins drawn with the same degree distribution. (C) Seed plus candidate HSP versus a matching set of proteins. (Left) Within group edge count (i.e., number of edges between members of the query set). (Middle) Interaction neighborhood overlap (i.e., Jaccard similarity). (Right) Network random walk similarity.

mice display defects of the periaxonal cytoplasmic collar in the spinal cord with later oligodendrocyte degeneration (34). MAG was found mutated in family 1226, displaying a homozygous Cys⁴³⁰→Gly⁴³⁰ missense mutation.

REEP2 encodes the receptor expression-enhancing protein 2, a paralog of *REEP1*, mutated in *SPG31* (35). Family 1967 displays a homozygous Met¹→Thr¹ mutation in *REEP2* removing

the canonical start codon and is mutated in a second recessive HSP family in an independent cohort (36). All of these gene mutations segregated with the phenotype in the family according to recessive inheritance and were not encountered in our exome database, consistent with pathogenicity. Although further validation of these three candidates is necessary in larger cohorts, the data suggest the HSPome can be

useful to identify HSP-relevant pathways and genes.

Link Between HSP and Neurodegenerative Disease Genes

Some of the genes we identified in this cohort have been previously associated with other neurodegenerative disorders (e.g., *CLN8*, *EIF2B5*, and *AMPD2*) primarily affecting areas of the nervous system other than the corticospinal tract. Prompted by this observation, we used the network to examine the similarity of HSP genes (seed + candidates) to other common neurological disorders. By using the random walk distance, we found that the set of HSP seeds plus candidates is significantly overlapping with sets of genes previously implicated in three neurodegenerative disorders, amyotrophic lateral sclerosis (ALS), Alzheimer's disease, and Parkinson's disease ($P = 1.1 \times 10^{-02}$, $P = 7.6 \times 10^{-03}$, $P = 1.6 \times 10^{-02}$, respectively) (Fig. 4). In contrast, we did not find a similar association with sets for representative neurodevelopmental disorders such as autism spectrum disorders and epilepsy ($P = 0.49$ and $P = 0.51$, respectively; fig. S12), nor with nonneurological disorders represented by heart and pulmonary disorders.

Discussion

By using WES, we identified 18 previously unknown candidates for AR-HSP (fig. S13), three of which (*ERLIN1*, *KIF1C*, and *NT5C2*) alone explain almost 20% of this cohort. These new candidates are predicted to display near 100% risk of HSP when mutated (37). All mutations were predicted as damaging to protein function, probably resulting in null or severely reduced function, consistent with the recessive mode of inheritance. In about 25% of the families a single candidate gene mutation could not be identified, probably a result of two factors: (i) Some mutations are in noncoding regions. (ii) Some causative mutations within the exome do not stand out more than other variants.

Four of our candidate HSP genes are located within previously identified loci for AR-HSP for which genes were not known: *ENTPDI*, *NT5C2*, *ERLIN1*, and *MARS*. Both *ERLIN1* and *NT5C2* are in the *SPG45* locus (38) and *ENTPDI* resides in *SPG27* (39). Recently, the *MARS2* gene, encoding a methionyl-tRNA synthetase, was implicated in the spastic ataxia 3 (*SPAX3*) phenotype (40). *KIF1C* is within the spastic ataxia 2 (*SAX2*) locus (41). On the basis of our findings, we returned to the original *SPAX2* family and identified a homozygous deletion of exons 14 to 18, confirming *KIF1C* as the *SPAX2* gene (fig. S14).

Our data support the idea that rare genetic mutations may converge on a few key biological processes, and our HSP interactome demonstrates that many of the known and candidate HSP genes are highly connected. This highlights important biological processes, such as cellular transport, nucleotide metabolism, and synapse and axon development. Some of the HSP gene modules suggest potential

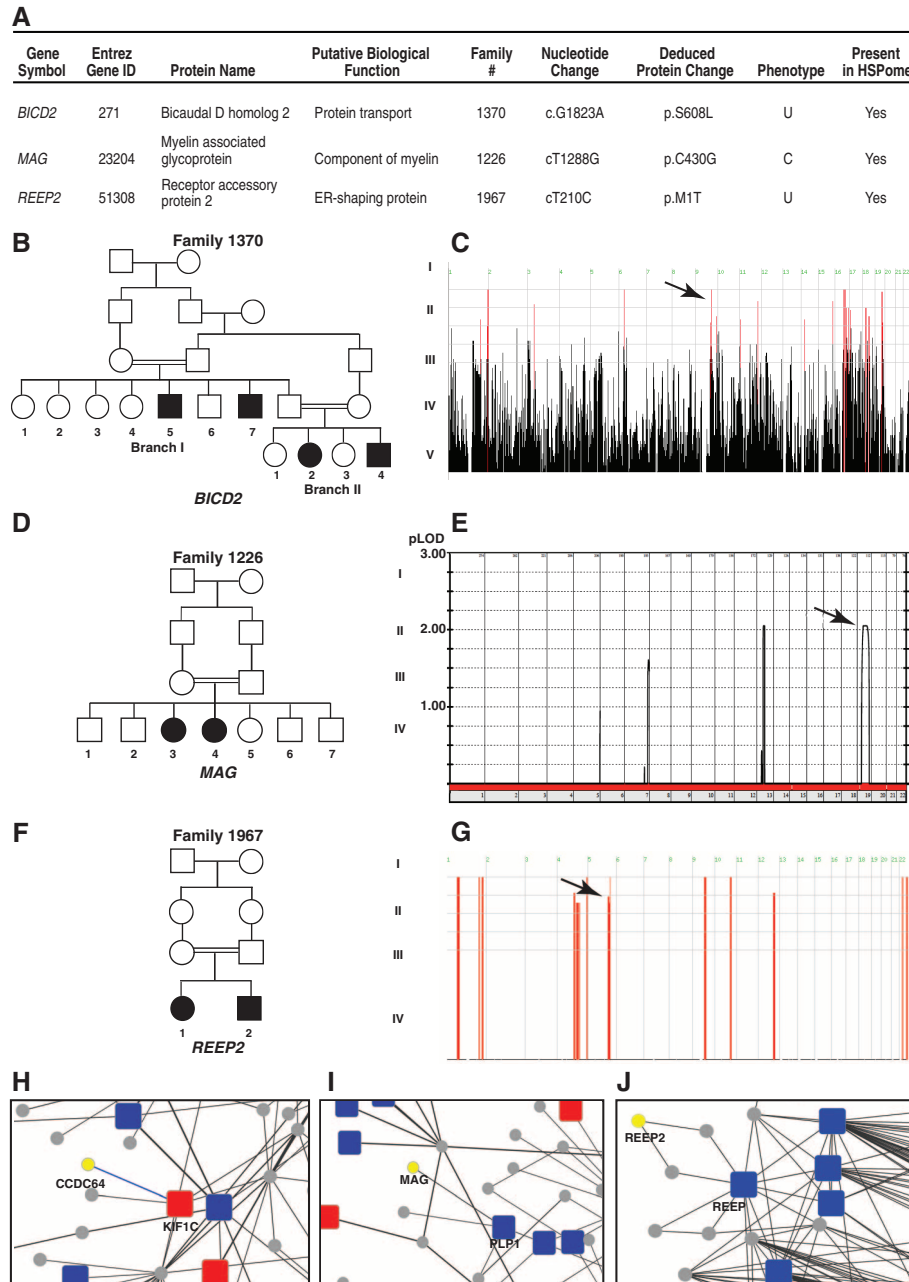


Fig. 3. Genes from HSP networks found mutated in HSP. (A) HSP candidate genes predicted from the HSPome found mutated in the HSP cohort. *BICD2*, *MAG*, and *REEP2* were subsequently found mutated in HSP families 1370 (B), 1226 (D), and 1967 (F), respectively. (C) Homozygosity plot from family 1370. Red bars, regions of homozygosity; arrow, homozygous block containing *BICD2*. (E) Linkage plot of family 1226; arrow, *MAG* locus. (G) Homozygosity plot; arrow, *REEP2* locus. (H to J) Zoom in from HSPome for specific interaction identifying candidates *CCDC64* (a paralog of *BICD2*), *MAG*, and *REEP2* (yellow) with previously published (blue) and newly identified (red) genes mutated in HSP. Blue lines denote manually curated interactions.

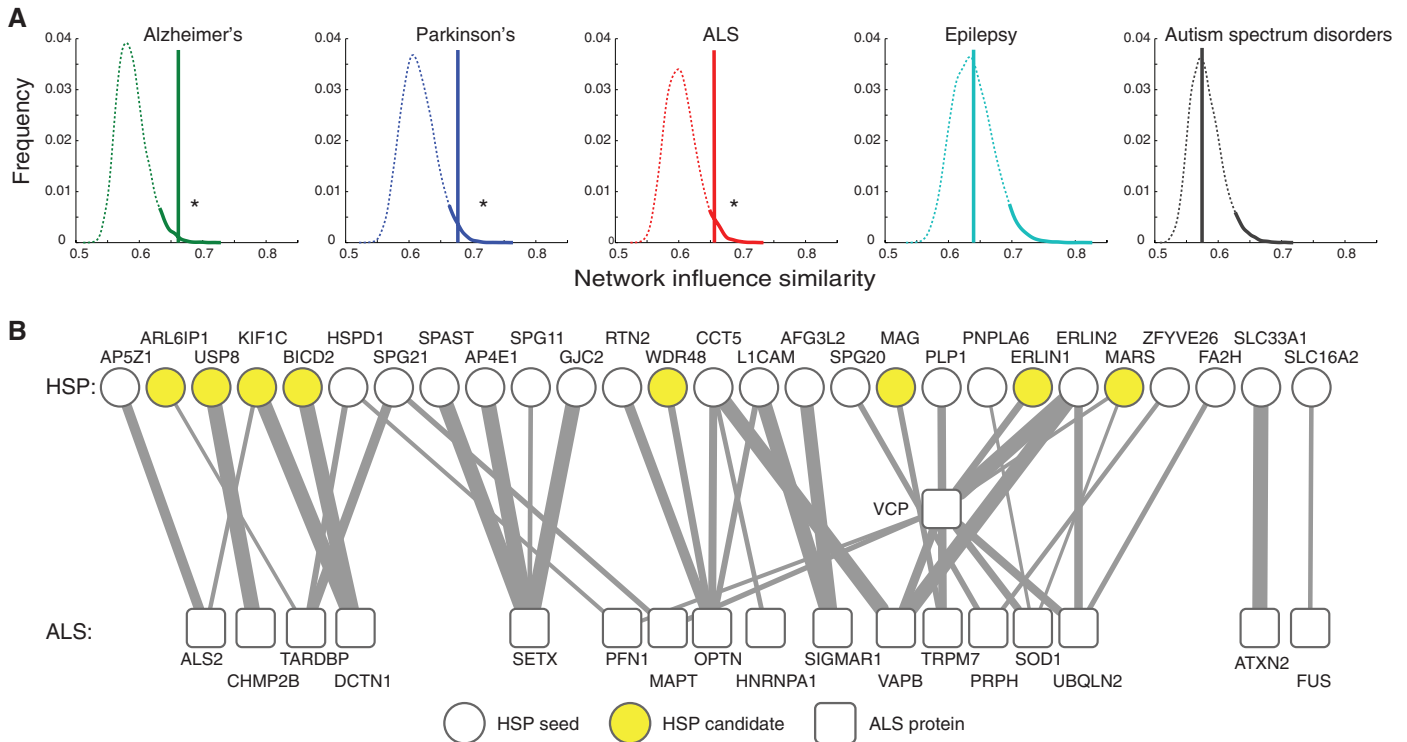


Fig. 4. Functional link between HSP genes and genes of other neurodegenerative conditions. (A) Density distribution representing random walk distances of OMM-derived neurodegeneration gene networks along with 10,000 permutations of randomly selected protein pools compared with the HSP seeds plus candidates pool. The top 5% distance is shaded. Only for Parkinson's, Alzheimer's, and ALS do the HSP seeds plus candidates fall within this 5%, whereas epilepsy and autism spectrum disorder show no statistical overlap. **(B)** Bipartite network showing the top links between the set of HSP and ALS proteins. Clear circles, HSP seeds; yellow circles, HSP candidates; boxes, ALS genes (VCP and ALS2 are implicated as causative of both HSP and ALS); line thickness, diffusion similarity between the two proteins.

points of treatment; for example, the nucleotide metabolism module or the lipid metabolism module could be targeted by bypassing specific metabolic blocks. Our HSPome ranked list of genes also provides candidates for unsolved cases of HSP. In addition to our analysis, we were able to link HSP with more common neurodegenerative disorders, indicating that the study of one disorder might advance the understanding of other neurodegenerative disorders as well.

Our study supports the principle that integrating family-based gene discovery together with prior knowledge (represented here as known causative genes and pathways) can facilitate the identification of biological pathways and processes disrupted in disease. Furthermore, this mode of analysis should be highly useful in the future to aid in the validation of private mutations in genes found in single families, to identify novel candidate genes and pathways, and for the discovery of potential therapeutic targets.

References and Notes

1. C. Blackstone, *Annu. Rev. Neurosci.* **35**, 25–47 (2012).
2. D. Seelov, M. Schuelke, F. Hildebrandt, P. Nürnberg, *Nucleic Acids Res.* **37**, W593–W599 (2009).
3. See supplementary text available on Science Online.
4. A. D'Amico *et al.*, *Neurology* **62**, 2138–2139 (2004).
5. C. Tesson *et al.*, *Am. J. Hum. Genet.* **91**, 1051–1064 (2012).
6. J. H. Schuurs-Hoeijmakers *et al.*, *Am. J. Hum. Genet.* **91**, 1073–1081 (2012).
7. C. Fassier *et al.*, *Nat. Neurosci.* **13**, 1380–1387 (2010).
8. F. Vandin, E. Upfal, B. J. Raphael, *J. Comput. Biol.* **18**, 507–522 (2011).

9. I. Lee, U. M. Blom, P. I. Wang, J. E. Shim, E. M. Marcotte, *Genome Res.* **21**, 1109–1121 (2011).
10. D. Szklarczyk *et al.*, *Nucleic Acids Res.* **39**, D561–D568 (2011).
11. O. Vanunu, O. Magger, E. Ruppin, T. Shlomi, R. Sharan, *PLOS Comput. Biol.* **6**, e1000641 (2010).
12. G. C. DeLuca, G. C. Ebers, M. M. Esiri, *Neuropathol. Appl. Neurobiol.* **30**, 576–584 (2004).
13. N. Rismanchi, C. Soderblom, J. Stadler, P. P. Zhu, C. Blackstone, *Hum. Mol. Genet.* **17**, 1591–1604 (2008).
14. G. Montenegro *et al.*, *J. Clin. Invest.* **122**, 538–544 (2012).
15. Y. Yildirim *et al.*, *Hum. Mol. Genet.* **20**, 1886–1892 (2011).
16. G. K. Voeltz, W. A. Prinz, Y. Shibata, J. M. Rist, T. A. Rapoport, *Cell* **124**, 573–586 (2006).
17. M. H. Wright, I. Berlin, P. D. Nash, *Cell Biochem. Biophys.* **60**, 39–46 (2011).
18. J. Park *et al.*, *Immunity* **17**, 221–233 (2002).
19. M. A. Cohn, Y. Kee, W. Haas, S. P. Gygi, A. D. D'Andrea, *J. Biol. Chem.* **284**, 5343–5351 (2009).
20. C. Dörner *et al.*, *J. Biol. Chem.* **273**, 20267–20275 (1998).
21. S. M. Lee, L. S. Chin, L. Li, *J. Cell Biol.* **199**, 799–816 (2012).
22. G. Skibinski *et al.*, *Nat. Genet.* **37**, 806–808 (2005).
23. Y. Zivony-Elboum *et al.*, *J. Med. Genet.* **49**, 462–472 (2012).
24. B. Renvois *et al.*, *Mol. Biol. Cell* **21**, 3293–3303 (2010).
25. J. H. Lumb, J. W. Connell, R. Allison, E. Reid, *Biochim. Biophys. Acta* **1823**, 192–197 (2012).
26. A. P. Sagona *et al.*, *Nat. Cell Biol.* **12**, 362–371 (2010).
27. H. A. Jinnah, R. L. Sabina, G. Van Den Berghe, *Handb. Clin. Neurol.* **113**, 1827–1836 (2013).
28. N. Akizu *et al.*, *Cell* **154**, 505–517 (2013).
29. B. Thauerer, S. Zur Nedden, G. Baier-Bitterlich, *J. Neurochem.* **121**, 329–342 (2012).
30. H. Najmabadi *et al.*, *Nature* **478**, 57–63 (2011).
31. M. A. Schlager *et al.*, *EMBO J.* **29**, 1637–1651 (2010).
32. X. Li *et al.*, *EMBO J.* **29**, 992–1006 (2010).
33. E. C. Oates *et al.*, *Am. J. Hum. Genet.* **92**, 965–973 (2013).
34. Z. Cai *et al.*, *J. Peripher. Nerv. Syst.* **7**, 181–189 (2002).
35. S. Züchner *et al.*, *Am. J. Hum. Genet.* **79**, 365–369 (2006).
36. T. Esteves *et al.*, *Am. J. Hum. Genet.*, published online 31 December 2013 (10.1016/j.ajhg.2013.12.005).

37. J. R. Lupski, J. W. Belmont, E. Boerwinkle, R. A. Gibbs, *Cell* **147**, 32–43 (2011).
38. U. Dursun, C. Koroglu, E. Kocayoz Orhan, S. A. Ugur, A. Tolun, *Neurogenetics* **10**, 325–331 (2009).
39. I. A. Meijer *et al.*, *Ann. Neurol.* **56**, 579–582 (2004).
40. V. Bayat *et al.*, *PLOS Biol.* **10**, e1001288 (2012).
41. N. Bouslam *et al.*, *Hum. Genet.* **121**, 413–420 (2007).

Acknowledgments: We are grateful to the participating families. Supported by the Deutsche Forschungsgemeinschaft (G.N.); the Brain and Behavior Research Foundation (A.G.F.); NIH R01NS041537, R01NS048453, R01NS052455, P01HD070494, and P30NS047101 (J.G.G.); French National Agency for Research (G.S., A.D.); the Verum Foundation (A.B.); the European Union (Omics call, “Neuromics” A.B.); Fondation Roger de Spoelberch (A.B.); P41GM103504 (T.I.); “Investissements d’avenir” ANR-10-IAIHU-06 (to the Brain and Spine Institute, Paris); and Princess Al Jawhara Center of Excellence in Research of Hereditary Disorders. Genotyping services provided in part by Center for Inherited Disease Research contract numbers HHSN268200782096C, HHSN2682011000111, and N01-CO-12400. We thank the Broad Institute (U54HG003067 to E. Lander), the Yale Center for Mendelian Disorders (U54HG006504 to R. Lifton and M. Gunel), M. Liv for technical expertise, and E. N. Smith, N. Schork, M. Yahyaoui, F. Santorelli, and F. Darios for discussion. Data available at dbGaP (accession number phs000288). UCSD Institutional Review Board (070870) supervised the study. The authors declare no competing financial interests.

Supplementary Materials

www.sciencemag.org/content/343/6170/506/suppl/DC1
Materials and Methods
Supplementary Text
Figs. S1 to S15
Tables S1 to S6
References (42–52)

18 October 2013; accepted 11 December 2013
10.1126/science.1247363